Control of Redox Potential by Deprotonation of Coordinated 1*H*-Imidazole in Complexes of 2-(1*H*-Imidazol-2-yl)pyridine

by **Gilles Stupka**, **Ludovic Gremaud**, and **Alan F. Williams***

Department of Inorganic, Analytical and Applied Chemistry, University of Geneva, 30 quai Ernest Ansermet, CH-1211 Geneva 4
(phone: +41 22 379 6425; fax: +41 22 379 6830; e-mail: Alan.Williams@chiam.unige.ch)

Dedicated to Professor *André Merbach* on the occasion of his 65th birthday

Complexes $[ML_3]^{2+}$ of the bidentate ligand 2-(1*H*-imidazol-2-yl)pyridine were prepared with iron(II), cobalt(II), and ruthenium(II). The electronic spectra suggest the ligand to be a weaker σ-donor and π-acceptor than the closely related 2,2′-bipyridine. The complexes are readily deprotonated by addition of base, and the effect of the deprotonation is to lower the M^{III}/M^{II} redox potential by roughly 900 mV. This is roughly 75% of the drop observed for related complexes of 2,6-di-1*H*-imidazol-2-ylpyridine, and suggests the effect to be largely coulombic in origin.

Introduction. – Although 1*H*-imidazole is easily the most important N-containing ligand in biological systems, 1*H*-imidazole-containing ligands have been much less studied in abiotic coordination chemistry than the related pyridine ligands. However, 1*H*-imidazole is naturally a bifunctional ligand, possessing a pyrrolic N-atom in addition to the pyridinic N-atom, which acts as a donor to transition metals. This NH functionality is available for H-bonding, and may also be deprotonated. The H-bonding property has been intensively studied in connection with metalloporphyrins [1], and H-bonding of 1*H*-imidazole coordinated to an iron porphyrin has been shown to shift the redox potential of the metal center by some 60 mV [2], stabilizing the iron(III) oxidation state. Coordination of 1*H*-imidazole significantly lowers the pK_a value of the pyrrolic H-atom [3–7] by *ca.* 5–7 log units, allowing deprotonation to occur in weakly basic solution (pH 8–10). The resulting imidazolate can act as a bridging ligand, as is well known in superoxide dismutase [8] and in many synthetic systems [9–12]. A less explicitly studied effect of deprotonation is the change in the metal redox potential. We have shown recently [13][14] that the ligand 2,6-di-1*H*-imidazol-2-ylpyridine (**1**) forms stable complexes $[M(\mathbf{1})_2]^{2+}$ with a number of transition metals, and that these complexes are readily deprotonated in basic solution. For M = Co, Fe, and Ru, the potential of the M^{III}/M^{II} couple is lowered by roughly 1300 mV upon full deprotonation of the complex. We were interested to see whether this large effect is observed with other 1*H*-imidazole-containing ligands, and, if so, to what extent the change in redox potential is dependent on the number of 1*H*-imidazoles deprotonated. We report here our results for the complexes $[M(\mathbf{2})_3]^{2+}$, which have three potentially acid pyrrolic protons compared to four in $[M(\mathbf{1})_2]^{2+}$.

The ligand 2-(1*H*-imidazol-2-yl)pyridine (**2**) has been known for many years, but its chemistry has been relatively little studied in comparison with that of the closely

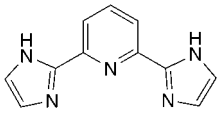

1

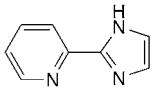

2

related 2,2′-bipyridine (bipy). *Chiswell*, *Lions*, and *Morris* [15] reported the syntheses of a number of complexes of **2** with a variety of M^{II} ions and noted that deprotonation occurred. *Eilbeck* and *Holmes* [16] a few years later reported the stability constants for the formation of complexes of **2** with M^{II} ions (M = Fe, Co, Ni, Cu, Zn, Cd, and Hg). *Boggess* and *Martin* [17] showed that the pyrrolic protons were indeed acidic in the complexes of formula $[M(\mathbf{2})_3]^{2+}$ (M = Fe, Co, Ni, Cu, and Zn) with pK_a values in the range 8–11. The complex $[Fe(\mathbf{2})_3]^{2+}$ has attracted a fair amount of attention, since it shows spin-crossover behavior in the solid state [18][19] and in solution [20–22]. A coordination polymer containing $[Fe(\mathbf{2})_2(4,4'\text{-bipy})]^{2+}$ repeat units was recently reported to show spin-crossover properties [23], and **2** was also used as a spectator ligand in the design of phosphatase model compounds [24]. To our knowledge, the only crystal structure of a complex of **2** is the coordination polymer $[Cu(\mathbf{2})(OH_2)(\text{dicyanamide})](NO_3)$ [25]. None of these publications discussed the electrochemistry, although *Baker* and *Goodwin* [19] noted that the deprotonation of $[Fe(\mathbf{2})_3]^{2+}$ led to the neutral low-spin iron(III) complex $[Fe(\mathbf{2}-H)_3]$. The electronic spectrum [26] and electrochemistry [27] of the complex $[Ru(\mathbf{2})_3]^{2+}$ have been reported, but no reference to possible deprotonation was made. The only case where the effect of deprotonation was discussed was $[Ru(bipy)_2(\mathbf{2})]^{2+}$, where *Haga* [28] reported that the deprotonation of ligand lowered the Ru^{III}/Ru^{II} potential by 380 mV. The current work reports the synthesis of the complexes $[M(\mathbf{2})_3]^{2+}$ (M = Fe, Co, Ni, and Ru) and the effect of deprotonation on the redox potentials. Some preliminary results on manganese complexes are also presented.

Results. – *Synthesis.* The complexes $[M(\mathbf{2})_3]^{2+}$ were generally prepared by simple mixing of alcoholic solutions of ligand with aqueous solutions of metal salt. Partial evaporation of the solution under vacuum followed by cooling gave the complex salts as microcrystalline solids, which were characterized by elemental analysis and electrospray mass spectroscopy. The Ru^{II} complex was prepared by refluxing $RuCl_3$ with a slight excess of **2** in ethylene glycol, followed by precipitation with ammonium hexafluorophosphate. The deprotonated complexes of Co^{III} and Fe^{III} were generated by addition of NaOH solution to solutions of $[M(\mathbf{2})_3]^{2+}$ whereupon the neutral complex $[M(\mathbf{2}-H)_3]$ precipitated; when applied to $[Ru(\mathbf{2})_3]^{2+}$, this gave a precipitate of $Na[Ru(\mathbf{2}-H)_3]$ showing that oxidation had not occurred. The $[Ni(\mathbf{2})_3]^{2+}$ complex showed a change in spectrum upon adding base, but the precipitate did not give a satisfactory analysis. Attempts to obtain manganese complexes were not successful. Mixing manganese(II) salts with ligand **2** gave solutions whose UV/VIS spectra were consistent with the formation of $[Mn(\mathbf{2})_3]^{2+}$ but addition of base gave dark green solutions that were unstable and gave precipitates of MnO_2. However, it was possible to

synthesize a higher-valence compound of manganese, $[Mn_2O_2(\mathbf{2})_4](ClO_4)_3$, following a method developed for bipyridine complexes [29].

UV/VIS Spectra. UV/VIS Spectra were recorded in MeOH. Ligand **2** shows two bands at 272 and 292 nm attributed to π-π* transitions. The complexes $[M(\mathbf{2})_3]^{2+}$ (M = Co, Ni) show these two bands slightly red-shifted together with the appearance of a new weaker band around 340 nm (*cf. Fig. 1*). The intensity of this band ($\varepsilon \approx 8000\ dm^3 \cdot mol^{-1} \cdot cm^{-1}$) and the fact that the position does not change greatly with change in the metal ion leads us to associate this with a ligand-centered transition, which is a useful marker of complexation of the ligand. Bands attributed to d-d transitions were observed at 974 nm (ε 6.7) for Co^{II} and 878 (ε 5) and 538 nm (ε 7) for Ni^{II}. These are red-shifted in comparison to the equivalent bipy complexes [30], indicating that **2** produces weaker ligand-field splitting than bipy, and consistent with the spin-crossover behavior of $[Fe(\mathbf{2})_3]^{2+}$ mentioned above [18–22]. The d^6 complexes of Ru^{II} and Fe^{II}) show the same ligand-based transitions, but any d-d bands are masked by strong absorption due to a metal-to-ligand charge transfer (MLCT) at 485 nm for Fe^{II} and 435 nm for Ru^{II} (*cf. Fig. 1*). This last value is close to that reported for this complex in aqueous solution [27]. For both metals, the MLCT band is blue-shifted in comparison to the analogous bipy complexes, where the band is observed at 532 nm (Fe^{II}) [30] and 452 nm [27]. The MLCT band for the Fe^{II} complex is less intense than for $[Fe(bipy)_3]^{2+}$ as a result of the spin-crossover behavior [20][31].

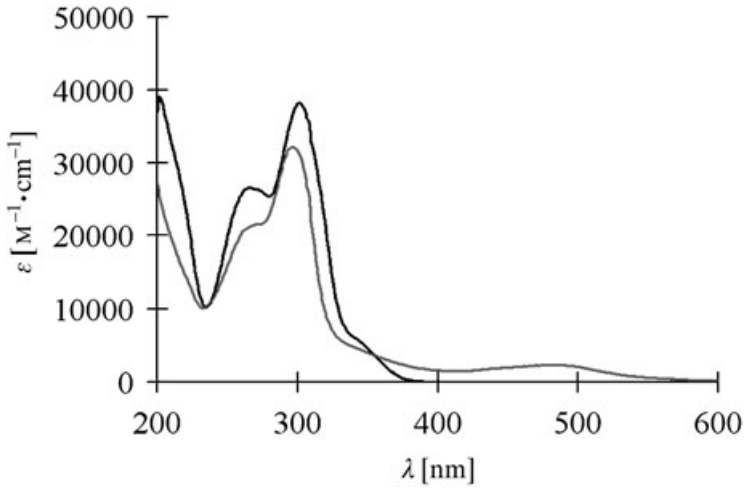

Fig. 1. *UV/VIS Spectra* (MeOH) *of* $[Ni(\mathbf{2})_3]^{2+}$ (black line) *and* $[Fe(\mathbf{2})_3]^{2+}$ (grey line) *showing the band at 350 nm indicating complexation of the ligand and the MLCT transition at 485 nm for the* Fe^{II} *complex*

Addition of base induces deprotonation. For the Ni^{II} complex, this results in a doubling of the intensity of the ligand-based band at 340 nm but in only a slight red shift of *ca.* 100 cm^{-1} of the d-d transitions, so we may assume that the ligand field is not changed significantly. For Co^{II}, we observe a decrease in the intensity of the ligand bands at 272 and 292 nm with a dramatic increase in the band at 340 nm. The d-d

transition at 974 nm disappears, consistent with the oxidation to Co^{III}. The Fe^{II} complex shows a behavior similar to that of the Co^{II} complex for the ligand-based transitions. The MLCT band disappears, and a new band, assigned to ligand-to-metal charge transfer (LMCT) for an Fe^{III} complex is observed at 739 nm. *Baker* and *Goodwin* reported a similar spectrum [19] for this complex and pointed out the disagreement with the spectrum reported by *Lions et al.* [15]. We suspect that this arises from only partial oxidation of Fe^{II} in the latter case. As we discuss below, the potential is lowered less than in the complex of ligand **1**, and it is possible that the isolated complex is contaminated with Fe^{II}, which has a higher extinction coefficient in the VIS than the Fe^{III} complex, and thus confers a red color on the solid. In support of this, the Ru^{II} complex (which has a similar redox potential, *vide infra*) does not undergo oxidation upon addition of base, but is deprotonated and gives a precipitate of $Na[Ru(\mathbf{2})_3]$. The spectrum of this deprotonated salt shows the usual increase in intensity at 340 nm, and the MLCT band is split into two bands at 423 and 469 nm.

The Mn^{II} complex gave a spectrum in which the appearance of a band at 340 nm indicates that complexation had taken place. Addition of base gave a dark green solution, suggesting that oxidation had occurred, but the solution was unstable and gave an intractable green precipitate. The complex $[Mn_2O_2(\mathbf{2})_4]^{3+}$ could be isolated as its perchlorate salt. The UV/VIS spectrum is very similar to that observed for the analogous bipy and phen complexes [29], but attempts to deprotonate the imidazole led to decomposition of the complex.

Isomers. Since **2** does not possess the full symmetry of 2,2′-bipyridine (bipy), complexes of the type $[M(\mathbf{2})_3]^{n+}$ exist as two isomers, *mer* (=(*OC*-6-21)) and *fac* (=(*OC*-6-22)). One would not expect any great difference in stablility between *mer* and *fac* isomers given the similar sizes and donor powers of the pyridine and imidazole moieties, and consequently one would expect a statistical value of 3:1 for the *mer*/*fac* ratio. This was observed for the similar complex tris(2-(1-methyl-1*H*-benzimidazol-2-yl)pyridine)cobalt(II) [32], where the kinetics of isomerization and the pressure dependence were studied, and the *mer/fac* isomerism of pyridinyl-1*H*-benzimidazole ligands around ruthenium was discussed recently by *Piguet* and collaborators [33]. In the present work, the ^{1}H-NMR spectrum of $[Ru(\mathbf{2})_3]^{2+}$ showed clearly a mixture of isomers. In the *mer* isomer, the three ligands are all inequivalent, giving a total of 18 different protons in the aromatic region, while, in the *fac* isomer, the C_3 axis makes all three ligands equivalent and gives six aromatic-proton signals. *Fig. 2* shows the aromatic region of the spectrum of $[Ru(\mathbf{2})_3]^{2+}$. The four *d* around 6.6 ppm are attributed to one of the imidazole protons, and integration indicates that the *mer*/*fac* ratio is close to the statistical value of 3:1. For most of the other complexes, the ^{1}H-NMR spectra were broadened by paramagnetic effects, and no information could be obtained, but, for $[Co(\mathbf{2}-H)_3]$, a well-resolved diamagnetic spectrum was observed, confirming the oxidation of Co^{II} to Co^{III}. In this case, the spectrum in the region of 6 ppm showed three peaks of equal intensity and one of *ca.* 20% of this intensity, implying a *mer*/*fac* ratio of *ca.* 15:1. Because of the statistical weighting in favor of the *mer* form, this corresponds to an energy difference of only a few kJ/mol. Following *Lever* [34], we assume that the *mer* and *fac* forms have essentially identical electronic spectra and electrochemistry.

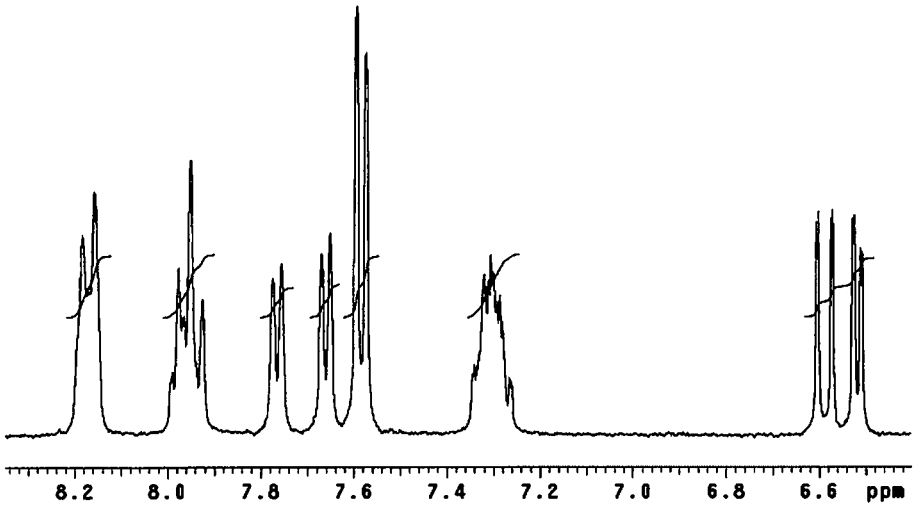

Fig. 2. *^{1}H-NMR Spectrum of [Ru(**2**)$_3$]$^{2+}$: the signals at* ca. *6.6 ppm may be used to quantify the* mer/fac *ratio* (see text)

Electrochemistry. – The cyclic voltammograms of the Co^{II}, Fe^{II}, and Ru^{II} complexes were studied, and the results are summarized in the *Table 1*. The Ni^{II} complex showed no observable electrochemical activity. The Fe^{II} and Ru^{II} complexes gave essentially reversible waves (*cf. Fig. 3*), but the Co peak separations were much greater. The potentials for the protonated complexes lie in the expected range. Thus, the potentials for $[M(\mathbf{2})_3]^{2+}$ (M = Co and Fe) are close to those reported for the related 2-(1-methyl-1*H*-benzimidazol-2-yl)pyridine complexes [35], and that for Ru^{II} is close to the value

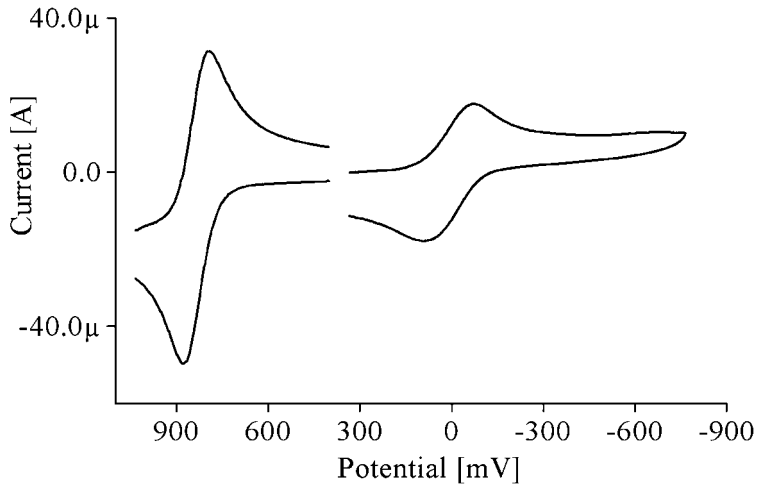

Fig. 3. *Cyclic voltammograms* (MeCN) *of [Fe(**2**)$_3$]$^{2/3+}$* (left) *and [Fe(**2** – H)$_3$]$^{-/0}$* (right)

Table. *Electrochemical Data Obtained by Cyclic Voltammetry* (MeCN) *for Complexes* $[M(\mathbf{2})_3]^{2+}$ *and the Deprotonated Complexes* $[M(\mathbf{2}-H)_3]^{-}$. Potentials are given with respect to the SCE. ΔE_p is the separation between anodic and cathodic peaks.

	Solvent	Ligand = **2**		Ligand = **2** – H		$\Delta E_{1/2}$/mV
		$E_{1/2}$/V	ΔE_p/mV	$E_{1/2}$/V	ΔE_p/mV	
Co	DMF	0.268	125	– 0.616	325	– 884
Fe	MeCN	0.835	81	0.004	139	– 831
Ru	DMF	0.836	91	– 0.083	125	– 919

previously reported in MeCN [27]. In general, the potentials are lower than for the equivalent bipy complexes but higher than those for the related complexes of ligand **1** [13][14]. This is in agreement with the observations of the MLCT bands discussed above. If one expresses the value for Ru^{II} relative to the NHE, a value for *Lever*'s electrochemical parameter [34] E_L of 0.18 is obtained.

Deprotonation of the complexes results in a dramatic drop in the potential for the M^{III}/M^{II} couple, consistent with the aerial oxidation of the complexes of Fe and Co. The average decrease is just under 900 mV, to be compared with a drop of 1250 mV observed upon deprotonation of $[M(\mathbf{1})_2]^{2+}$. The change is thus roughly proportional to the number of 1*H*-imidazole moieties complexed to the metal ion and corresponds to 300 mV per 1*H*-imidazole unit. This value may be compared to the drop of 60 mV estimated for H-bonding to 1*H*-imidazole in porphyrin systems [2] and is close to the value of 380 mV reported by *Haga* [28] for the effect of deprotonating $[Ru(bipy)_2(\mathbf{2})]^{2+}$. The *Lever* E_L value calculated for deprotonated **2** from the Ru complex is 0.02, corresponding in his classification to a weakly π-acid unsaturated amine [34].

The electrochemistry of the mixed-valence manganese complex $[Mn_2O_2(\mathbf{2})_4]^{3+}$ showed a signal corresponding to $Mn_2^{IV} \rightarrow Mn^{IV}Mn^{III}$ at + 1.21 V ($\Delta E_p = 131$ mV), slightly lower than the values for the phen and bipy complexes, in agreement with the general tendency observed for **2**. An irreversible wave attributed to the reduction to Mn^{III}_2 was observed just below 400 mV.

Discussion. – The results presented here confirm and complete the observations with ligand **1**. The observation that the drop in redox potential is roughly constant for each ligand, and proportional to the number of deprotonated 1*H*-imidazole moieties argues that the effect is due to the coulombic effect of building up negative charge on the ligand and thereby stabilizing a higher oxidation state for the complexed metal by a *Madelung* potential. As judged by the insignificant change in the position of the d-d bands for the Ni, the deprotonation does not greatly change the interaction of the ligand with the metal, and, if specific orbital effects were involved, we would expect more-significant differences in the effect of deprotonation between the d^5/d^6 iron and Ru couples, and the d^6/d^7 Co^{III}/Co^{II} couple.

In both ligands **1** and **2**, the 1*H*-imidazole ligand is bound to an aromatic moiety, and this may play an important role in stablizing the deprotonated 1*H*-imidazole. In support of this, deprotonation of histidine does not appear to take place readily in biological systems. The 1*H*-imidazole ligands studied by *Matsumoto* and co-workers [36][37] also

show deprotonation, but in this case the 1*H*-imidazole is bound to an imine functionality that also offers a means of delocalizing the negative charge generated by deprotonation of the 1*H*-imidazole. Preliminary experiments in our laboratory [38] suggest that deprotonation of the 1*H*-imidazole ligand coordinated to M^{II} ions does not occur when bound to purely aliphatic groups. If this is indeed the case, then this is unlikely to be an important mechanism for biological systems where the 1*H*-imidazole is attached to a saturated chain. Nonetheless, the coupling between protonation state of ligand **2** and the redox potential of the metal offers a possible switching mechanism controlled by pH.

We thank the *Swiss National Science Foundation* for the support of this work.

Experimental Part

General. Solvents and starting materials were purchased from *Fluka AG* (Buchs, Switzerland) and used without further purification, unless otherwise stated. MeCN and dimethylformamide (DMF) were distilled from CaH_2. Pyridine-2-carboxaldehyde was freshly distilled before use. UV/VIS Spectra: *Cary 1E* or *Perkin-Elmer Lambda-900* UV/VIS/NIR spectrometer; quartz cells of 0.1- and 0.01-cm path lengths; λ_{max} (ε) in nm. IR Spectra: *Perkin-Elmer Spectrum-One* instrument; KBr discs; NMR Spectra: *Varian Gemini-300* instrument; at 300 (^{1}H) and 74.44 MHz (^{13}C) at 20°; chemical shifts δ in ppm with respect to $SiMe_4$, *J* in Hz; the residual solvent δ(H) was used as a reference, *i.e.*, D_2O δ 4.80, CD_3CN δ 1.95, CD_3OD δ 3.31, CD_3Cl δ 7.26, and $((CD_3)_2SO$ δ 2.41), and δ(C) 67.4 of dioxane for D_2O solns. $\tilde{\nu}$ in cm^{-1}. MS: electron impact (EI) at 70 eV with *VG 7000E* and *Finnigan 4000* instruments, electrospray ionization (ESI) with *Finnigan Mat-SSQ-7000* instrument of the Mass Spectrometry Laboratory, University of Geneva; in *m*/*z* (rel. %). Elemental analyses were performed by Dr. *H. Eder*, University of Geneva.

Electrochemistry. Cyclic voltammograms were recorded by using a *BAS-CV-50W* potentiostat connected to a personal computer. A three-electrode system consisting of a stationary Pt-disk working electrode, a Pt counter electrode, and a nonaqueous Ag/AgCl reference electrode was used. Bu_4NPF_6 (0.1M) served as an inert electrolyte. Before each measurement, the system was standardized with the ferrocene/ferrocenium couple ($E_{1/2} = +0.50$ *vs.* SCE [39]) in DMF, and with $[Ru(bipy)_3](ClO_4)_2$ [40] in MeCN. Potentials are the mean of anodic and cathodic peaks and are given with respect to SCE.

*2-(1*H*-Imidazol-2-yl)pyridine* (**2**) [15][20]. A soln. of freshly distilled pyridine-2-carboxaldehyde (22.65 g, 0.21 mol) was added to a soln. of glyoxal (=ethanedial; 29 ml, 40% aq. soln.) in EtOH at 0°. Ice-cold concentrated aq. ammonia (85 ml) was rapidly added, and the mixture was stirred in an ice bath for 1 h and allowed to warm to r.t.. The mixture was extracted with Et_2O (10 × 100 ml), dried (Na_2SO_4), and evaporated. The residue was treated with charcoal in refluxing EtOH and recrystallized from MeOH: **2** (9 g, 30%). White solid. M.p. 135°. UV/VIS (MeOH): 272 (11900), 292 (15400). IR (KBr): *ca.* 3350*w*, 1614*s*, 1594*s*, 1568*w*, 1479*s*, 1458*s*, 1414*m*, 1381*m*, 1307*m*, 1280*m*, 1171*w*, 1135*m*, 1108*m*, 992*s*, 955*s*, 788*s*, 737*m*, 708*s*, 620*m*, 503*w*, 466*w*, 403*m*. ^{1}H-NMR (300 MHz, (D_6)DMSO): 8.58 (*d*, $^3J = 4.2$, 1 H); 8.03 (*d*, $^3J = 8.1$, 1 H); 7.86 (*td*, $J = 7.8, 1.5$, 1 H); 7.34 (*ddd*, $J = 7.5, 4.8, 1.5$, 1 H); 7.13 (*s*, 2 H). EI-MS: 145 (100, $M^{+\bullet}$).

*Tris[2-(1*H*-imidazol-2-yl-*κ*N^3)pyridine-*κ*N]cobalt(2+) Diperchlorate*[1]), ($[Co(\mathbf{2})_3](ClO_4)_2$). A soln. of $Co(ClO_4)_2 \cdot 6H_2O$ (0.336 g, 0.92 mmol) in H_2O (5 ml) was added to a soln. of **2** (0.40 g, 2.75 mmol) in EtOH (5 ml). The resulting orange soln. was concentrated and, upon cooling, an orange powder precipitated which was filtered and washed with Et_2O: $[Co(\mathbf{2})_3](ClO_4)_2$ (0.600 g, 94%). UV/VIS (MeOH): 268 (26300), 293 (32400), 974 (6.7). IR (KBr): 3244*m*, 3158*m*, 2934*m*, 1613*s*, 1571*m*, 1472*s*, 1295*m*, 1103 (br.), 965*m*, 929*m*, 794*s*, 751*m*, 704*s*, 623*s*, 483*w*, 415*w*, 383*w*, 264*w*. ESI-MS (MeOH): 174.9 ($[Co(\mathbf{2})_2]^{2+}$, 100), 246.9 ($[Co(\mathbf{2})_3]^{2+}$, 15). Anal. calc. for $[Co(\mathbf{2})_3](ClO_4)_2 \cdot H_2O$: C 40.52, H 3.25, N 17.72; found: C 40.82, H 3.51, N 17.89.

*Tris[2-(1*H*-imidazol-2-yl-*κ*N)pyridine-*κ*N]iron(2+) Diperchlorate*[1]) ($[Fe(\mathbf{2})_3](ClO_4)_2$). A soln. of $Fe(ClO_4)_2 \cdot 6H_2O$ (0.417 g, 1.15 mmol) in H_2O (5 ml) was added to a soln. of **2** (0.50 g, 3.45 mmol) in MeOH (5 ml). The resulting red soln. was concentrated, and upon cooling, a purple powder precipitated which was

[1]) **Caution**: Dry perchlorates may explode and should be handled in small quantities and with the necessary precautions [41].

filtered and washed with Et_2O: $[Fe(\mathbf{2})_3](ClO_4)_2$ (0.706 g, 89%). UV/VIS (MeOH): 265 (21200), 295 (32100), 485 (2350). IR (KBr): 3250 (br.), 3158*w*, 1614*s*, 1567*m*, 1471*s*, 1450*m*, 1294*m*, 1103 (br.), 964*m*, 930*m*, 788*s*, 753*s*, 703*s*, 623*s*, 504*w*, 455*w*, 411*w*, 384*w*. ESI-MS (MeOH): 173.3 ($[Fe(\mathbf{2})_2]^{2+}$, 55, 245.9 ($[Fe(\mathbf{2})_3]^{2+}$, 30). Anal. calc. for $[Fe(\mathbf{2})_3](ClO_4)_2 \cdot H_2O$): C 40.70, H 3.27, N 17.79; found: C 40.74, H 3.53, N 17.86.

*Tris[2-(1*H*-imidazol-2-yl-*κ*N^3)pyridine-*κ*N]nickel(2+) Bis(tetrafluoroborate)* ($[Ni(\mathbf{2})_3](BF_4)_2$). A soln. of $Ni(BF_4)_2 \cdot 6H_2O$ (0.622 g, 1.83 mmol) in H_2O (5 ml) was added to a soln. of **2** (0.80 g, 5.5 mmol) in EtOH (5 ml). The resulting violet soln. was concentrated, and, upon cooling, a pink-violet powder precipitated, which was filtered and washed with Et_2O: $[Ni(\mathbf{2})_3](BF_4)_2$ (0.855 g, 70%). UV/VIS (MeOH): 264 (26400), 300 (38000), 538 (7), 878 (5). IR (KBr): 3302 (br.), 3159*w*, 2939*w*, 1615*s*, 1572*m*, 1493*m*, 1472*s*, 1295*m*, 1071 (br.), 964*m*, 930*m*, 794*s*, 753*s*, 704*s*, 640*m*, 521*m*, 422*w*, 386*w*, 280*w*. ESI-MS (MeOH): 174.2 ($[Ni(\mathbf{2})_2]^{2+}$, 100), 246.7 ($[Ni(\mathbf{2})_3]^{2+}$, 25). Anal. calc. for $[Ni(\mathbf{2})_3](BF_4)_2 \cdot H_2O$: C 42.03, H 3.38, N 18.38; found: C 42.13, H 3.70, N 18.45.

*Tris[2-(1*H*-imidazol-2-yl-*κ*N^3)pyridine-*κ*N]ruthenium(2+) Bis(hexafluorophosphate)*. ($[Ru(\mathbf{2})_3](PF_6)_2$). A mixture of **2** (0.344 g, 2.37 mmol) and $RuCl_3$ (0.150 g, 0.72 mmol) was refluxed in ethylene glycol (30 ml) for 1 h. The soln. was cooled to r.t., H_2O (30 ml) added, and the product precipitated with a conc. aq. NH_4PF_6 soln. The red-orange complex was filtered and washed with H_2O: $[Ru(\mathbf{2})_3](PF_6)_2$ (0.416 g, 70%). UV/VIS (MeOH): 294 (43460), 435 (13800). IR (KBr): 3386*m*, 1614*m*, 1495*s*, 1469*s*, 1163*m*, 1115*m*, 1102*m*, 840 (br.), 782*m*, 751*m*, 702*m*, 558*s*, 397*w*, 348*w*, 301*w*. ^{1}H-NMR (300 MHz, (D_6)DMSO): 8.17 (*d*, $^3J = 7.8$, 4 H); 7.95 (*m*, 4 H); 7.76 (*d*, $^3J = 5.4$, 2 H); 7.66 (*d*, $^3J = 5.7$, 2 H); 7.59 (*d*, $^3J = 0.9$, 2 H); 7.57 (*d*, $^3J = 0.9$, 2 H); 7.30 (*m*, 4 H); 6.60 (*d*, $^3J = 1.2$, 1 H); 6.57 (*d*, $^3J = 1.2$, 1 H); 6.53 (*d*, $^3J = 1.2$, 1 H); 6.51 (*d*, $^3J = 1.2$, 1 H). ESI-MS (MeOH): 268.4 ($[Ru(\mathbf{2})_3]^{2+}$, 100). Anal. calc. for $[Ru(\mathbf{2})_3](PF_6)_2$: C 34.87, H 2.56, N 15.25; found: C 34.88, H 3.23, N 15.20.

*Tris[2-(pyridin-2-yl-*κ*N)-1*H*-imidazolato-*κ*N^1]cobalt* ($[Co(\mathbf{2}-H)_3]$). To a soln. of $[Co(\mathbf{2})_3](ClO_4)_2$ (0.15 g, 0.21 mmol) in a minimum of MeOH was added 0.84M aq. NaOH (1 ml, 4 equiv.): The resulting red-brown soln. was cooled to 0° and the precipitated red powder was filtered and washed with Et_2O: $[Co(\mathbf{2}-H)_3]$ (0.082 g, 80%). UV/VIS (MeOH): 264 (21100), 291 (17000), 346 (19600). IR (KBr): 1612*s*, 1558*m*, 1519*s*, 1462*m*, 1447*m*, 1427*m*, 1344*m*, 1215*m*, 1144*m*, 1103*m*, 984*m*, 758*s*, 522*m*, 467*m*, 416*w*, 401*w*, 301*w*, 277*w*. ^{1}H-NMR (300 MHz, (D_6)DMSO): 8.05–7.95 (*m*); 7.90 (*d*); 7.83 (*d*); 7.20–7.33 (*m*); 7.18 (*s*); 7.15 (*s*); 7.07 (*s*); 7.03 (*s*); 6.78 (*d*); 6.66 (*d*); 6.19 (*s*); 5.97 (*s*); 5.87 (*s*); 5.71 (*s*). EI-MS : 491 ($[Co(\mathbf{2}-H)_3]$, 65), 347 ($[Co(\mathbf{2}-H)_2]$, 55), 203 ($[Co(\mathbf{2}-H)]$, 9), 145 (L, 100). Anal. calc. for $[Co(\mathbf{2}-H)_3] \cdot 3/2\,H_2O$: C 55.60, H 4.08, N 24.31; found: C 55.75, H 4.46, N 24.40.

*Tris[2-(pyridin-2-yl-*κ*N)-1*H*-imidazolato-*κ*N^1]iron* ($[Fe(\mathbf{2}-H)_3]$). To a soln. of $[Fe(\mathbf{2})_3](ClO_4)_2$ (0.15 g, 0.21 mmol) in a minimum of MeOH was added 0.29M aq. Et_3N (3 ml, 4 equiv.). The resulting red-violet soln. was cooled to 0° and the precipitated red-violet powder filtered and washed with Et_2O: $[Fe(\mathbf{2}-H)_3]$ (0.092 g, 90%). UV/VIS (MeOH): 289 (23900), 331 (21800), 739 (730). IR (KBr): 1611*s*, 1558*m*, 1519*s*, 1449*s*, 1393*m*, 1283*m*, 1203*m*, 1160*m*, 1101*m*, 984*m*, 781*s*, 756*s*, 710*s*, 505*w*, 455*m*, 438*m*, 411*m*, 385*w*, 301*w*. Anal. calc. for $[Fe(\mathbf{2}-H)_3] \cdot 2\,H_2O$: C 54.97, H 4.22, N 24.04; found: C 55.30, H 4.54, N 24.22.

*Sodium Tris[2-(pyridin-2-yl-*κ*N)-1*H*-imidazolato-*κ*N^1]ruthenium(1−)* ($Na[Ru(\mathbf{2}-H)_3]$). To a soln. of $[Ru(\mathbf{2})_3](PF_6)_2$ (0.1 g, 0.12 mmol) in a minimum of MeOH was added 0.48M aq. NaOH (1 ml, 4 equiv.). The resulting brown soln. was filtered and cooled to 0°, and the precipitated red-brown powder filtered and washed with Et_2O: $Na[Ru(\mathbf{2}-H)_3]$ (0.046 g, 69%). UV/VIS (MeOH): 298 (33200), 423 (8150), 469 (6480). IR (KBr): 3385 (br.), 1603*s*, 1550*m*, 1501*s*, 1456*m*, 1328*m*, 1145*m*, 1099*m*, 972*m*, 937*m*, 779*s*, 751*m*, 710*m*, 642*m*, 508*m*, 450*w*, 399*m*, 340*w*, 300*w*. ^{1}H-NMR (300 MHz, CD_3OD): 7.82 (*m*, 4 H); 7.73 (*d*, $^3J = 5.4$); 7.66 (*d*, $^3J = 5.7$); 7.62 (*d*, $^3J = 5.4$); 7.52 (*m*); 7.09 (*s*, 1 H); 7.08 (*s*, 1 H); 7.07 (*s*, 1 H); 7.05 (*s*, 1 H); 6.8 (*m*, 4 H); 6.43 (*s*, 1 H); 6.37(*s*, 1 H); 6.36 (*s*, 1 H). ESI-MS (MeOH): 534.1 ($[Ru(\mathbf{2}-H)_3]^-$, 30). Anal. calc. for $[Ru(\mathbf{2}-H)_3] \cdot Na \cdot H_2O \cdot 1/4$ MeOH: C 49.92, H 4.15, N 21.77; found: C 49.99, H 3.63, N 21.64.

*Tetrakis[2-(1*H*-imidazol-2-yl-*κ*N^3)pyridine-*κ*N]di-μ-oxo-dimanganese(3+) Triperchlorate*[1]) ($[Mn^{III}Mn^{IV}O_2(\mathbf{2})_4](ClO_4)_3$). To a soln. of $[Mn(OAc)_2 \cdot 4H_2O$ (0.169 g, 0.69 mmol) in H_2O (2.5 ml) was added **2** (0.3 g, 2.07 mmol) in EtOH (2 ml). Acetate buffer (4 ml) was added. The yellow soln. was cooled to 0° in an ice bath and $KMnO_4$ (0.047 g, 0.3 mmol) in H_2O (2 ml) was added dropwise. The resulting green soln. was stirred for 15 min at 0° and filtered. Conc. $NaClO_4$ soln. was added to precipitate the product as a green powder, which was filtered and washed with Et_2O and Et_2O: $[Mn^{III}Mn^{IV}O_2(\mathbf{2})_4](ClO_4)_3$ (0.12 g, 24%). IR (KBr): 3567*m*, 3094*w*, 2756*w*, 1615*m*, 1571*m*, 1474*s*, 1294*m*, 1103 (br.), 971*m*, 928*w*, 790*s*, 747*m*, 703*s*, 655*m*, 624*s*, 411*w*, 366*w*, 279*w*. ESI-MS (MeCN): 295.6 ($[Mn_2O_2(\mathbf{2})_4(MeCN)_4]^{3+}$, 70), 281.9 ($[Mn_2O_2(\mathbf{2})_4(MeCN)_3]^{3+}$, 20%). Anal. calc. for $[Mn_2O_2](\mathbf{2})_4(ClO_4)_3 \cdot 2\,H_2O$: C 36.36, H 3.03, N 15.90; found: C 36.28%, H 3.23, N 15.84.

REFERENCES

[1] R. Quinn, J. Mercer-Smith, J. N. Burtstyn, J. S. Valentine, *J. Am. Chem. Soc.* **1984**, *106*, 4136.
[2] P. O'Brien, D. A. Sweigart, *Inorg. Chem.* **1985**, *24*, 1405.
[3] T. R. Harkins, H. Freiser, *J. Am. Chem. Soc.* **1954**, *78*, 1143.
[4] G. C. Hayward, H. A. O. Hill, J. M. Pratt, R. J. P. Williams, *J. Chem. Soc. A* **1971**, 196.
[5] J. M. Harrowfield, V. Norris, A. M. Sargeson, *J. Am. Chem. Soc.* **1976**, *98*, 7282.
[6] M. F. Hoq, R. E. Shepherd, *Inorg. Chem.* **1984**, *23*, 1851.
[7] C. R. Johnson, W. W. Henderson, R. E. Shepherd, *Inorg. Chem.* **1984**, *23*, 2754.
[8] D. Bordo, A. Pesce, M. Bolognesi, M. E. Stroppolo, M. Falconi, A. Desideri, in 'Handbook of Metalloenzymes', Eds. A. Messerschmidt, R. Huber, T. Poulos, and K. Wieghardt, Wiley, Chichester – New York – Weinheim – Brisbane – Singapore – Toronto, 2001.
[9] P. V. Bernhardt, G. A. Lawrance, N. J. Curtis, *Polyhedron* **1987**, *6*, 1347.
[10] C. Piguet, B. Bocquet, E. Müller, A. F. Williams, *Helv. Chim. Acta* **1989**, *72*, 323.
[11] R. Quinn, M. Nappa, J. S. Valentine, *J. Am. Chem. Soc.* **1982**, *104*, 2588.
[12] N. Matsumoto, Y. Motoda, T. Matsuo, T. Nakashima, N. Re, F. Dahan, J.-P. Tuchagues, *Inorg. Chem.* **1999**, *38*, 1165.
[13] R. F. Carina, L. Verzegnassi, G. Bernardinelli, A. F. Williams, *Chem. Commun.* **1998**, 2681.
[14] G. Stupka, G. Bernardinelli, A. F. Williams, *Dalton Trans.* **2004**, 407.
[15] B. Chiswell, F. Lions, B. S. Morris, *Inorg. Chem.* **1964**, *3*, 110.
[16] W. J. Eilbeck, F. Holmes, *J. Chem. Soc. A* **1967**, 1777.
[17] R. K. Boggess, R. B. Martin, *Inorg. Chem.* **1974**, *13*, 1525.
[18] R. J. Dosser, W. J. Eilbeck, A. E. Underhill, P. J. Edwards, C. E. Johnson, *J. Chem. Soc. A* **1969**, 810.
[19] A. T. Baker, H. A. Goodwin, *Aust. J. Chem.* **1977**, *30*, 771.
[20] K. A. Reeder, E. V. Dose, L. J. Wilson, *Inorg. Chem.* **1978**, *17*, 1071.
[21] E. V. Dose, M. A. Hoselton, N. Sutin, M. F. Tweedle, L. J. Wilson, *J. Am. Chem. Soc.* **1978**, *100*, 1141.
[22] J. K. Beattie, K. J. McMahon, *Aust. J. Chem.* **1988**, *41*, 1315.
[23] G. S. Matouzenko, G. Molnar, N. Bréfuel, M. Perrin, A. Bousseksou, S. A. Borshch, *Chem. Mater.* **2003**, *15*, 550.
[24] F. Verge, C. Lebrun, M. Fontecave, S. Ménage, *Inorg. Chem.* **2003**, *42*, 499.
[25] J. Carranza, C. Brennan, J. Sletten, F. Lloret, M. Julve, *J. Chem. Soc., Dalton Trans.* **2002**, 3164.
[26] J. G. D. M. Atton, R. D. Gillard, *Transition Met. Chem.* **1995**, *6*, 351.
[27] G. Orellana, M. L. Quiroga, A. M. Braun, *Helv. Chim. Acta* **1987**, *70*, 2073.
[28] M. Haga, *Inorg. Chim. Acta* **1983**, *75*, 29.
[29] S. R. Cooper, M. Calvin, *J. Am. Chem. Soc.* **1977**, *99*, 6623.
[30] R. A. Palmer, T. S. Piper, *Inorg. Chem.* **1966**, *5*, 864.
[31] K. A. Reeder, E. V. Dose, L. J. Wilson, *Inorg. Chem.* **1978**, *17*, 1071.
[32] L. J. Charbonnière, A. F. Williams, U. Frey, A. E. Merbach, P. Kamalaprija, O. Schaad, *J. Am. Chem. Soc.* **1997**, *119*, 2488.
[33] S. Torelli, S. Delahaye, A. Hauser, G. Bernardinelli, C. Piguet, *Chem.–Eur. J.* **2004**, *10*, 3503.
[34] A. B. P. Lever, *Inorg. Chem.* **1990**, *29*, 1271.
[35] L. J. Charbonniére, A. F. Williams, C. Piguet, G. Bernardinelli, E. Rivara-Minten, *Chem.–Eur. J.* **1998**, *4*, 485.
[36] I. Katsuki, Y. Motoda, Y. Sunatsuki, N. Matsumoto, T. Nakashima, M. Kojima, *J. Am. Chem. Soc.* **2002**, *124*, 629.
[37] Y. Sunatsuki, Y. Ikuta, N. Matsumoto, H. Ohta, M. Kojima, S. Iijima, S. Hayami, Y. Maeda, S. Kaizaki, F. Dahan, J.-P. Tuchagues, *Angew. Chem., Int. Ed.* **2003**, *42*, 1614.
[38] M. Bergamo, N. Banerji, G. Bernardinelli, A. F. Williams, unpublished results.
[39] J. C. Chambron, C. Coudret, J. P. Sauvage, *New J. Chem.* **1992**, *16*, 361.
[40] A. J. Bard, L. R. Faulkner, 'Electrochemical Methods: Fundamentals and Applications', Wiley, New York, 1980.
[41] W. C. Wolsey, *J. Chem. Educ.* **1978**, *55*, A355.

Received November 12, 2004